

# New emission phase of the Be/X-ray binary X Persei: nearly simultaneous spectroscopic and near-infrared observations

Q.Z. Liu<sup>1,2</sup>, H.R. Hang<sup>1</sup>

<sup>1</sup> Purple Mountain Observatory, Nanjing 210008, China: National Astronomical Observatories, Chinese Academy of Sciences

<sup>2</sup> Astronomical Institute "Anton Pannekoek", University of Amsterdam, Kruislaan 403, 1098 SJ Amsterdam, The Netherlands

Received 4 December 1999 / Accepted 15 August 2000

**Abstract.** We present a series of optical spectroscopic and near-infrared photometric observations of the Be star X Persei, from the beginning of the recent emission phase. Our data show that after the latest extended low state (*ELS*), both the equivalent width (*EW*) of the H $\alpha$  emission line and the *JHK* luminosities gradually increased. The recent maximum H $\alpha$  *EW* and *JHK* magnitudes are more than but comparable to the 1986-1989 maxima, which reflects a more extensive and denser envelope in the new emission phase.

The IR photometry and the H $\alpha$  *EW* increase coincidentally in the early stage of the new emission phase. However, the variations in the following years, especially in 1994 and 1995, are much different from the early variations. An unusual variation that while the H $\alpha$  *EW* in X Per increases considerably, the *JHK* magnitudes decline rapidly is seen in our nearly simultaneous spectroscopic and near-infrared observations.

An expanding ring model is put forward to interpret the observed unusual variations between the H $\alpha$  *EW* and near-IR luminosity during the recent emission phase of X Persei. Our results indicate that although both infrared excess and H $\alpha$  emission line arise from the envelope, their main contributors, in some cases, are likely to originate in the different part of the envelope.

**Key words:** stars : Be stars– X-ray : binariesstars : individual : X Persei

## 1. Introduction

X Persei, the optical counterpart of the X-ray source 4U0352+30 (Braes & Miley 1972), is a sixth magnitude B0 Ve star (Lyubimkov et al. 1997; Roche et al. 1997) with a magnetized neutron star companion (pulse period 835s). Possible orbital period of the system is 580 days, detected in the radial velocities of the Balmer lines (Hutchings 1977). This period has not yet been confirmed, and is even doubted (Penrod & Vogt 1985; Reynolds et al. 1992).

The star is also a known optical variable on time scales from minutes to years.

X Persei sometimes showed extreme, extended low states (Mook et al. 1974; Roche et al. 1993). Optical and near infrared photometry indicated that X Persei dropped to an extreme low state begun in 1989 March (Norton et al. 1991; Roche et al. 1993). During this period the H $\alpha$  line profile changed from emission to absorption, accompanied by a decrease in the IR flux by over a magnitude (Norton et al. 1991; Reynolds et al. 1992; Roche et al. 1993). This behavior indicated the loss of the circumstellar disk around the Be star as is also known from single Be star. This opportunity has been used for determining the physical parameters of the primary star (Fabregat et al. 1992; Lyubimkov et al. 1997). Corbet & Thomas (1991) reported the H $\alpha$  line in emission again in October 1991, which meant that a new circumstellar disk began to form. More recently, Zamanov & Zamanova (1995) found the optical low state at *V* band begun in the mid-1990 had ended in the spring of 1993. The system reached maximum brightness in late 1994, and has subsequently entered a period of relatively rapid fading. The most comprehensive optical and IR variations of X Per over the past decades, covered the latest *ELS*, were presented by Roche et al. (1993; 1997) and Telting et al. (1998). The spectral observations in Feb. 1995 showed the He I  $\lambda$  6678 was in emission with quadruple peaks, implying the existence of a double disc structure (Tarasov & Roche 1995; Kunjaya & Hirata 1995).

In this paper, we present the nearly simultaneous optical spectroscopy and near-IR photometry of this interesting object from the beginning of the new emission phase. It is a good opportunity to trace the build-up of a new envelope and the subsequent evolution of the new envelope in X Persei. Some early observations were reported in a previous paper (Liu & Hang 1997). Finally, we will put forward a model to give an explanation of the observed phenomenon between the H $\alpha$  *EW* and near-IR luminosity.

**Table 1.** Near-IR measurements of X Persei/4U0352+30.

Date	Julian date (-2440000)	J (1.25 $\mu$ m)	H (1.25 $\mu$ m)	K (1.25 $\mu$ m)
92.11.11	8938.18	6.51	6.54	6.51
92.11.18	8945.33	6.56	6.30	6.54
93.11.07	9299.26	6.01	5.71	5.44
94.09.17	9614.29	5.56	5.40	5.10
94.09.19	9616.30	5.32	5.26	5.19
94.09.20	9617.34	5.60	5.47	5.32
94.09.22	9619.31	5.45	5.32	5.26
95.11.07	10029.33	6.23	6.23	6.08
95.11.11	10033.28	6.17	6.15	6.01

## 2. Observations and results

Since the autumn of 1992, we have chosen a set of Be stars, especially Be/X-ray binaries, for spectroscopic and near-IR luminosity monitoring. X Persei was one of the program stars. All observations were carried out at Xinglong station of Beijing Astronomical Observatory and at Yunnan Astronomical Observatory.

### 2.1. Near-IR photometry

The near-IR photometry was measured at Xinglong station of Beijing Astronomical Observatory by using the 1.26 m reflectors with a liquid nitrogen cooled InSb photometer covering the *JHK* bands. Typical errors are  $\pm 0.05$  for *J*, *H* bands, and  $\pm 0.07$  for *K* band. The results of measurements are presented in Table I.

Fig. 1 shows the observed IR lightcurves of X Persei in the *JHK* bands, together with the results from Norton et al. (1991), Reynolds et al. (1992), Roche et al. (1993), and Telting et al. (1998). For comparison we also collect the published data of the optical *V* magnitude during the same period (Zamanov & Zamanova 1995) and include them in the figure. One can see that the brightness in *JHK* was almost constant during the *ELS*, at a level of *J*, *H* and *K* approximate to 6.6 magnitude. The *ELS* ended with a gradual increase in brightness, reaching a flat high state peaked around JD 2449700, in agreement with the optical data. The peak *V* magnitude recovered its 1986-1989 maximum brightness of 6.2<sup>m</sup>, with an increase of  $\Delta V \approx 0.6^m$  over the magnitude at the latest *ELS*. All the lightcurves show a similar pattern, and the IR brightness variations follow those of the V-band lightcurve, but with greater amplitude:  $\Delta J \approx 1.3^m$ ,  $\Delta H \approx 1.4^m$ ,  $\Delta K \approx 1.5^m$ . This recent maximum is of comparable brightness, in all IR bands, to the 1986-1989 maximum. The observations in October 1995, however, showed a rapid fall to *J* = 6.2<sup>m</sup>, *H* = 6.1<sup>m</sup>, *K* = 6.0<sup>m</sup>, close to the magnitudes at the *ELS*.

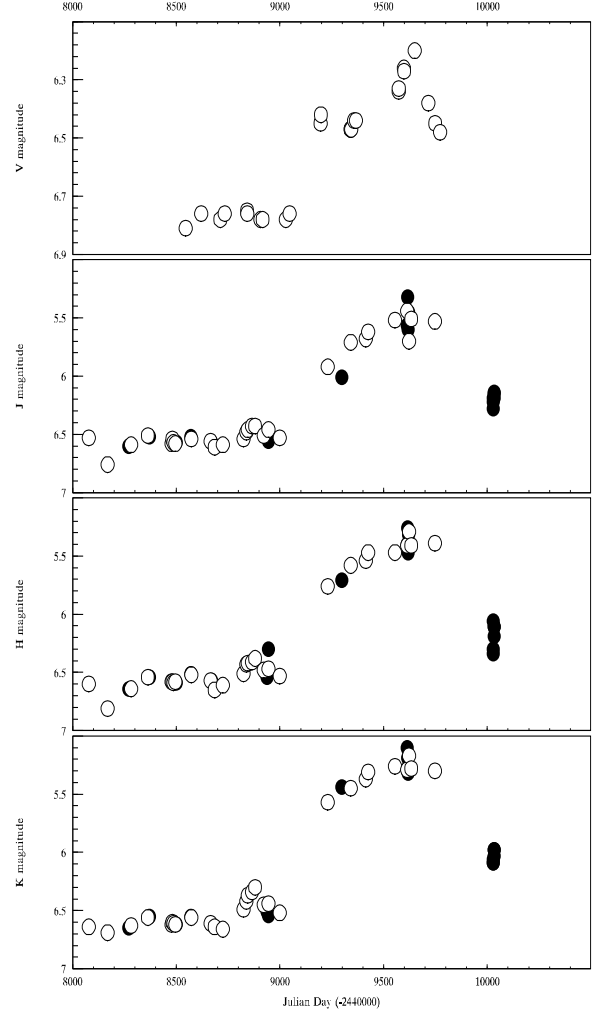


**Fig. 1.** The near-IR *JHK* magnitudes during the course of the monitoring programme. Open circles are from Roche et al. (1993), Norton et al. (1991), Reynolds et al. (1992), and Telting et al. (1998); filled circles are from this work.

### 2.2. Optical spectroscopy

The optical spectroscopic observations were mainly made at Xinglong station of Beijing Astronomical Observatory with a CCD grating spectrograph at the Cassegrain focus of the 2.16 m telescope. Two additional high-resolution spectra were performed at the Coude focus of the 100cm telescope at Yunnan Astronomical Observatory. The journal of the observations for X Per is summarized in Table II, together with the *EW* of H $\alpha$  and HeI 6678 lines. Sometimes the object was observed several times at one night. He- Ar spectra were taken in order to obtain the pixel-wavelength relations. All spectroscopic data are reduced with IRAF software on our Sun-4 station except the spectra taken in 1992, which were reduced with FIGARO/DIPSO software on the Vax 11/780 computer of

Purple Mountain Observatory. They are bias subtracted and flat field corrected. The influence of night sky light on the spectra has been eliminated.

Spectroscopic observations of X Per show that the emission line profiles are highly variable. They are characterized by strong emission features of H Balmer and HeI lines. Fig. 2 shows the development of the emission-line profiles for the H $\alpha$  and HeI  $\lambda$ 6678 between 1992 and 1998. All the profiles have been normalized to neighboring continuum. We respectively show several representative H $\alpha$  and HeI  $\lambda$ 6678 line spectra from our total data set. Three of respectively H $\alpha$  and HeI  $\lambda$ 6678 spectra were taken during the rise to maximum brightness (which occurred around 1994 November), and five H $\alpha$  and four HeI  $\lambda$ 6678 spectra during the subsequent fade. The line measurements of H $\alpha$  and HeI  $\lambda$ 6678 for the double-peaked profiles are summarized in Table III, with intensity above continuum ( $I$ ), peak separation ( $\Delta v_p$ ) between  $V$  and  $R$  components, and the outer envelope radius ( $R_s$ ) deduced from  $\Delta v_p$  (Huang 1972) listed.

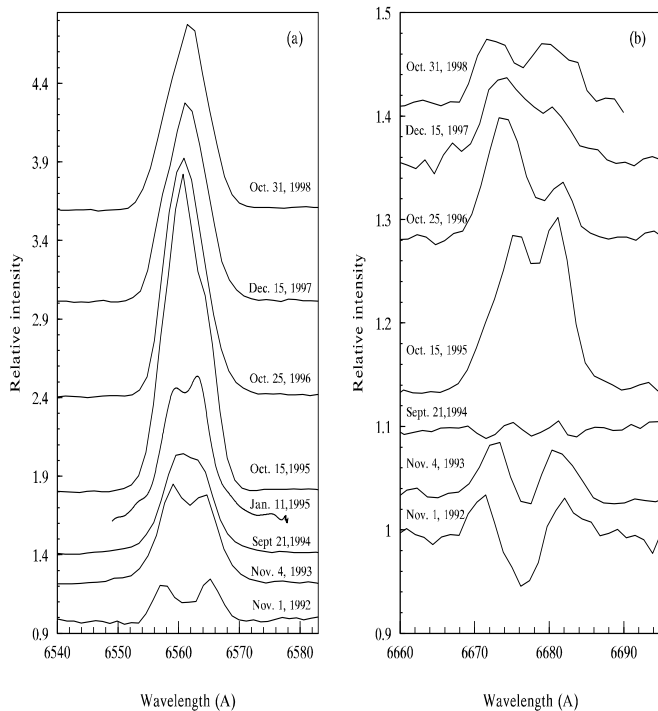


**Fig. 2.** Series of the H $\alpha$  spectra (a) and the HeI  $\lambda$ 6678 spectra (b) of X Persei during 1992-1998. All spectra have had the continuum level normalized and are annually offset vertically to allow direct comparison. Note the asymmetric H $\alpha$  profile in Oct. 1995, the significant decrease of the HeI  $\lambda$ 6678 line intensity in 1994 and the asymmetric profile in 1996 and 1997.

The H $\alpha$  spectra (Fig. 2a) during the first three years showed a well-defined double peak with that the intensity

of  $V$  component is nearly equal to that of  $R$  component. The intensity enhancement was concentrated on the central parts of the line between two emission peaks with the peak separation gradually reduced. Such variations can be explained by the gradual expansion of the new envelope away from X Persei and/or the dissipation of the envelope (Hang & Xia 1995; Liu & Hang 1997). The line did not further increase and was still weak at the peak JHK magnitudes in 1994, but began to increase again in early 1995 with an asymmetric profile ( $I_V / I_R \approx 0.9$ ). The line intensity reached maximum in October 1995, and then gradually decreased over a few years with a single peak profile. The  $V$  and  $R$  components initially separated by  $\sim 378 \text{ km s}^{-1}$  in the 1992 spectrum, but narrowing to  $\sim 168 \text{ km s}^{-1}$  in early 1995.

Fig. 2b shows that the HeI  $\lambda$ 6678 line, after increasing during the first two years of the recent emission phase, almost disappeared in October 1994, with only a faint double peak ( $EW = 0.07 \text{ \AA}$ ) superposed on the photospheric absorption line. In October 1995, however, there were large increases in both the blue and red peaks, as well as in the wings. While the line splitting in the H $\alpha$  had almost disappeared and a strong asymmetry was visible, the HeI  $\lambda$ 6678 still remained a well-defined double peak. The four peaks in 1995 February spectra reported by Tarasov & Roche (1995), however, did not find in our 1995 October data. The features are narrow, so maybe the medium resolution spectra that we have simply do not resolve the multiple peaks (Roche, private communication). The HeI line in 1992 spectrum had broad  $V$  and  $R$  wings, with a separation of  $\sim 477 \text{ km s}^{-1}$ . This evolved to a narrower line profile ( $v_p \sim 274 \text{ km s}^{-1}$ ) in 1994. We note that the shape of the He I line throughout these years is always double-peaked, and the two peaks differ very little in intensity, exception for the 1996 and 1997 spectra.

The H $\alpha$   $EW$  varies more gradually than  $V$  and  $JHK$  magnitudes. Fig. 3 shows the H $\alpha$   $EW$  (lower panel) and  $J$  magnitude (upper panel) as a function of time. Some H $\alpha$   $EW$  data are from Roche et al. (1993) and Kunjaya & Hirata (1995). From the accumulated data one can see that the increase of the H $\alpha$   $EW$  started earlier than the brightening in the near-infrared  $J$  magnitude. It began to increase at JD 2448600 while the optical  $V$  and near-infrared  $JHK$  magnitudes were still at extremely low level. The dramatically increasing  $EW$  is immediately apparent with the H $\alpha$   $EW$  changing from  $-0.2 \text{ \AA}$  in 1992 to  $-16.3 \text{ \AA}$  in 1995. It is interesting to note that the  $EW$  in 1994 did not increase to its peak, as the  $J$  magnitude did. Its  $EW$  was only  $-6.5 \text{ \AA}$  at the peak  $J$  magnitude, not much different from its value in 1993. The H $\alpha$   $EW$ , however, was seen to dramatically increase during the optical and near-infrared fade. While the latter got fainter dramatically, the  $EW$  increased rapidly, reaching a peak value of  $-16.3 \text{ \AA}$  in October 1995. This value exceeds the maximum value of  $-14.1 \text{ \AA}$  known just before the latest

**Table 2.** Journal of the spectroscopic observations of X Persei/4U0352+30.

Date	Julian date (-2440000)	Dispersion (Å/mm)	Resolution (Å/pixel)	H $\alpha$ <i>EW</i> (Å)	HeI 6678 <i>EW</i> (Å)
92.11.01	8928.2	101	2.26	-0.93	0.18
92.11.03	8930.1	101	2.26	-1.39	0.16
92.11.04	8931.2	101	2.26	-1.45	0.16
93.11.04	9296.2	50	1.39	-6.41	-0.29
93.11.07	9299.1	50	1.39	-6.35	-0.23
94.09.21	9618.2	50	1.22	-6.68	0.07
95.01.11	9729.1	- -	0.0478	-10.45	- - -
95.10.15	10006.3	50	1.22	-16.02	-1.59
95.10.17	10008.3	50	1.22	-16.34	-1.79
96.10.25	10382.3	50	1.22	-12.43	-1.00
96.10.26	10383.2	50	1.22	-12.59	-1.07
97.12.15	10798.2	50	1.22	-10.60	-0.78
97.12.16	10799.2	50	1.22	-10.92	-0.92
97.12.18	10801.2	50	1.22	-11.58	-1.09
98.10.31	11118.2	50	1.22	-9.706	-0.60

**Table 3.** Main parameters of the selected spectra of the H $\alpha$  and HeI  $\lambda$ 6678 lines of X Persei.

Date	Julian date (-2440000)	H $\alpha$				HeI 6678	
		$I_V$	$I_R$	$\Delta v_p$ (km s $^{-1}$ )	$R_s(R_*)$	$\Delta v_p$ (km s $^{-1}$ )	$R_s(R_*)$
92.10.30	8926.3	1.20	1.25	378.	1.12	477.	0.70
93.11.07	9297.3	1.65	1.61	254.	2.48	312.	1.64
94.09.21	9618.3	1.66	1.66	167.	5.74	274.	2.13
95.01.11	9729.0	1.86	1.86	158.	6.41	- - -	- - -
95.10.15	10006.3		3.03	single peak		273.	2.15
96.10.25	10382.3		2.52	single peak		384.	1.09
97.12.15	10799.3		2.27	single peak		274.	2.13
98.10.31	11118.3		2.17	single peak		330.	1.47

*ELS*, and to our best knowledge, is also the highest value ever recorded.

### 2.3. Correlation between the infrared magnitude and the H $\alpha$ *EW*

It is generally accepted (Neto & Pacheco 1984; Ashok et al. 1984) that the same electrons that produce the excess continuum emission in the infrared are also responsible for the hydrogen emission lines which are a characteristic of the Be stars. In addition, the observed correlation between the H $\alpha$  and near-infrared fluxes of Be stars served as direct evidence of the coincidence of the IR and Balmer line emitting regions (Neto & Pacheco 1984; Ashok et al. 1984; van Kerkwijk, Waters, & Marlborough 1995).

The correlation between the nearly simultaneous infrared  $J_{ELS}-J$  magnitude and the H $\alpha$  *EW* in X Persei is shown in Fig. 4. Some additional data are from Norton et al. (1991), Reynolds et al. (1992), and Roche et al. (1993). We find that a positive correlation is existence for the values at the early stage of the recent emission phase, consistent with the results reported by Dachs &

Wamsteker (1982) and Roche et al. (1993). The observations of 1994 and 1995, however, fell well off this trend. We will put forward a model in the next section to give a qualitative explanation for this unusual phenomenon.

### 3. The expanding ring model

The observed IR excesses have been generally attributed to free-free and free-bound emission from envelopes around Be stars. Since the emission due to recombination declines rapidly for highly excited states, free-free emission dominates the IR spectrum (Chokshi & Cohen 1988; Kastner & Mazzali 1989). The free-free emission coefficient is given by

$$j_{\nu}^{ff} = 6.842 \times 10^{-38} N_i N_e T^{-1/2} Z g_{ff} e^{-\frac{h\nu}{kT_e}}, \quad (1)$$

in erg/cm $^3$ /s/Hz, where  $g_{ff}$  is the free-free Gaunt factor,  $Z$  is the charge,  $T$  is the temperature of the gas in  $^{\circ}$ K,  $N_e$  and  $N_i$  are electron and ion densities in cm $^{-3}$ . The opacity is then obtained via Kirchoff's Law, giving

$$\kappa_{\nu}^{ff} = 3.692 \times 10^8 N_i N_e T^{-1/2} \nu^{-3} g_{ff} (1 - e^{-\frac{h\nu}{kT_e}}), \quad (2)$$

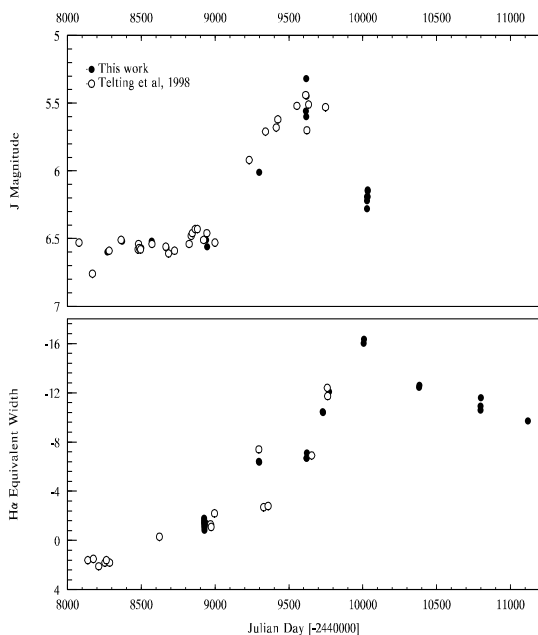


**Fig. 3.** The equivalent width of H $\alpha$  emission line and  $J$  magnitude over the course of the monitoring programme. H $\alpha$   $EW$  data are from Roche et al. (1993) and Kunjaya & Hirata (1995) (open circles); and from this work (filled circles)

for the free-free absorption coefficient. The H $\alpha$  recombination-line intensity is given by (Tucker, 1975)

$$j_{H\alpha} = 1.0265 \times 10^{-24} N_i N_e T^{-1/2} \ln\left(\frac{h\nu_0}{kT}\right), \quad (3)$$

in erg/cm<sup>3</sup>/s, where  $\nu_0$  is the frequency at the Lyman limit. The absorption coefficient at the center of H $\alpha$  line is given by (Osterbrook, 1989)

$$\kappa_{H\alpha} = \frac{\pi e^2}{m_e c \Delta\nu_D} f_{23} N_{0,2} \left[1 - e^{-\frac{h\nu_{23}}{kT}}\right], \quad (4)$$

where  $f_{23}$  is the oscillator force,  $N_{0,2}$  is the volume density of atoms excited in the level 2,  $\Delta\nu_D$  is the Doppler width of the line defined by thermal motions, and the other parameters refer to the usual physical constants.

### 3.1. The slab model

In order to interpret the unusual variations between the near-infrared excess and the H $\alpha$   $EW$ , we consider a model in which the equatorial matter ejected from the primary is an expanding ring with a total mass of  $M_1$  and an initial ring width of  $L_1$ . We assume the ring is expanding following the polytropic law:

$$TV^{n-1} = T_1 V_1^{n-1} = \text{const}, \quad (5)$$

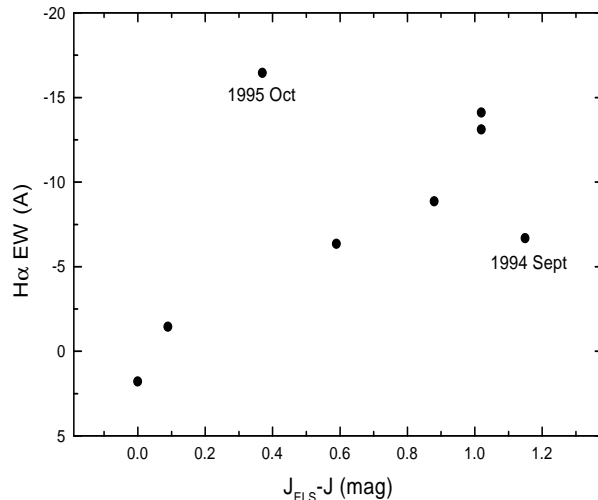


**Fig. 4.** The correlation between  $J_{ELS} - J$  magnitude and equivalent width of the H $\alpha$  emission line in X Persei

where  $n$  is the polytropic index,  $T$  is temperature,  $V$  is volume. The subscript '1' denotes the value at the surface of stellar photosphere ( $r = 1R_*$ ). The temperature and density of the gas ring is  $r$ -related and decreases as the ring expanded, but at a given radius, the temperature and density are assumed to be uniform. We further assume that the width of the ring depends upon  $r$  as  $L(r) = L_1 r^m$ .

Considering a pure hydrogen envelope viewed with an angle  $i$ , we will calculate the luminosities from H $\alpha$  line emission ( $L_{H\alpha}$ ) and from infrared continuum in the  $J$  band ( $L_J$ ) according to this model, by taking optical depth into account. We assume the envelope confined to a slab disc with a thickness  $D(= 2H)$ . In some recent models, a cone disc with an opening angle of  $\theta = 5^\circ$  was taken (Marlborough, Zijlstra & Waters 1997); Telting et al. (1998). However, this does not change the results fundamentally.

### 3.2. The model parameters and results

The double peaks at H $\alpha$  in our spectra in the strong emission phase imply that  $i$  is not so small, while no report concerning shell lines suggests that  $i$  is not close to  $90^\circ$ . We adopt  $i = 30^\circ$  in terms of the derived stellar mass of  $15.5 M_\odot$ , stellar radius of  $7 R_\odot$  and  $v \sin i$  of  $200 \text{ km s}^{-1}$  (Lyubimkov et al. 1992).

We adopt an effective temperature  $T_{eff}$  of  $30000^\circ\text{K}$ , a radius  $R_* = 7R_\odot$ , and a gravitational acceleration  $\log g = 4.0$  for X Persei, because they were derived during the latest disk-less phase (Lyubimkov et al. 1992). Referring to Waters et al. (1988), the density distribution for Be/X-ray binaries is given by  $N(r) = N_1 r^{-n_d}$  with index  $n_d$  between 2 and 3.75. We take  $n = 7/6$  and  $m = 2$ , so that the density and temperature distributions are  $N(r) = N_1 r^{-3}$

and  $T = T_1 r^{-1/2}$  (Waters 1986) with  $N_1$  and  $T_1$  taken to be  $10^{13} \text{ cm}^{-3}$  and  $30000^\circ\text{K}$ , respectively. The thickness of the slab is assumed  $H = 0.2R_*$ .

With these numerical values taken, we can obtain the variations of the luminosities of the  $\text{H}\alpha$  emission line and infrared continuum in the present model as a function of radius. The results are shown in Fig. 5 with the luminosities normalized to their maximum values.

Fig. 5 illustrates that the near-infrared continuum emission changes dramatically with its peak between  $1R_*$  and  $2R_*$ . It increases to its maximum value rapidly and so does the subsequent decrease. The near infrared emission is almost concentrated on the regions within the radius of  $2R_*$ , which is well consistent with the result obtained by Persi et al. (1977). The variation of the  $\text{H}\alpha$  emission, however, is more gradual. The emission slowly increases with radius as the ring outwardly expands and dissipates. The  $\text{H}\alpha$  emission reaches maximum much later than the near-infrared emission does. When the  $\text{H}\alpha$  emission reaches its maximum value around radius  $r = 6R_*$ , the near-infrared emission is almost disappeared.

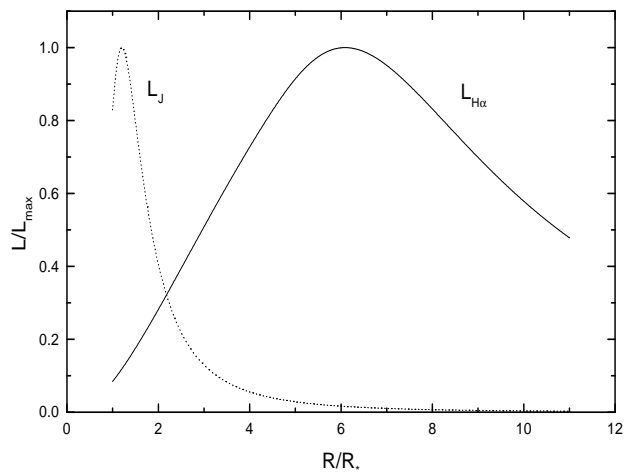


**Fig. 5.** The luminosity of  $\text{H}\alpha$  line emission and infrared continuum emission as a function of radius, for the model with initial density of  $10^{13} \text{ cm}^{-3}$  and temperature of  $30000^\circ\text{K}$ . Other parameters are taken to be  $H = 0.2R_*$ ,  $n = 7/6$ ,  $m = 2$ , and  $i = 30^\circ$

The overall pattern (Fig. 5) is in agreement with the observational data shown in Fig. 3. However, we wish to emphasize here that the results obtained in this section are still preliminary. They need to be regarded with caution in view of the many assumptions necessary to derive them.

#### 4. Discussion

Fig. 2 shows that the intensities of the  $\text{H}\alpha$  emission line in 1993 and 1994 spectra did not change much while He I line clearly fell. This implies that the envelope has begun to dissipate. Hence, the large increase started in early 1995 indicates that, during 1994, before the old envelope dissipated completely, a new and larger one has begun to be generated. The four-peak structure in the He I profile, observed a little later, clearly showed the coexistence of the two envelopes.

The successive record of the  $\text{H}\alpha$  activity from the beginning of the new emission phase of X Persei permits us to trace the evolution of the envelope in some detail. The basic pattern is as follows: at first, the envelope was fed with matter, and the  $\text{H}\alpha$  emission intensity evolved from zero to a definite value, implying the beginning of the new emission phase. After having developed over a few years, by 1994, the envelope began to decay on a longer time-scale. The fading process, however, was interrupted by a new, major outburst. At this time the former contributed mainly to the  $\text{H}\alpha$  *EW* and only slightly to the *JHK*, while the latter gave large near-infrared excesses but contributed little to  $\text{H}\alpha$ , due to its proximity to the photosphere with a large optical depth. Thus the observed  $\text{H}\alpha$  *EW* and *JHK* magnitudes can be produced. Thereafter, as the primary cease to eject matter and the ejected matter moved outwards, an envelope ring was formed. The outward motion of the new ring resulted in the decrease of the optical depth of the envelope ring due to the rapidly reduced density. When the ring reached several  $R_*$ , a strong  $\text{H}\alpha$  and small infrared excess were produced (see Fig. 5). Meanwhile, the old one still generated small  $\text{H}\alpha$  *EW* and *JHK* magnitudes, and so were produced the high *EW* of  $\text{H}\alpha$  and faint *JHK* magnitudes. We suggest that the coexistence of the two rings may also be one of the factors for both the  $\text{H}\alpha$  *EW* and peak *JHK* magnitudes exceeded their previous peak values.

For some Be stars, the  $\text{H}\alpha$  profiles did not change much over times (e.g.  $\alpha$  Ara, etc.), and this may be related to a steady ejection of matter; for some others, the  $\text{H}\alpha$  profiles underwent rapid changes (e.g.  $\mu$  Cen; Hanuschik et al. 1993), and this may be related to occasional ejection. For steady ejection that leads to a steady disk-like envelope, there may exist a linear relation between the infrared excess and  $\text{H}\alpha$  *EW*, whereas for transient ejection that leads to ring-shaped envelope, such a linear relation may not exist. We suggest that the variations in X Persei in recent years are intermediate: the early stage of the new emission phase is dominated by the early stage of a steady ejection while the later stage is likely to be related to a sporadic ejection.

#### 5. Conclusions

We present the nearly simultaneous optical spectroscopic and near-infrared photometric observations of the Be star

X Persei, the optical counterpart to the X-ray source 4U0352+30. Our data show that the *JHK* magnitudes and  $H\alpha$  *EW* in the new phase increase to high levels that exceeded the maximum values ever recorded. The observed high value of the *EW* and *JHK* magnitudes may reflect a more extensive and denser envelope in the new emission phase.

The infrared photometry and the *EW* of  $H\alpha$  emission line increase coincidentally in the early stage of the new emission phase, consistent with the results by Roche et al. (1993) for X Persei and by Dachs & Wamsteker (1982) for  $\mu$  Cen,  $\omega$  Ori and HD58343. However, the variations for the observations in 1994 and 1995, are largely deviated from the trend. The  $H\alpha$  *EW* hardly enhanced at the peak *JHK* magnitudes in 1994, but it is seen to dramatically increase during the optical and near-infrared fade. While the latter got fainter dramatically, the *EW* increased rapidly, reaching a maximum of  $-16.34 \text{ \AA}$  in October 1995.

We put forward a model in which the circumstellar envelope is an expanding ring, to interpret the unusual relation between the  $H\alpha$  *EW* and near infrared luminosities observed during the recent emission phase of X Persei. We suggest that the unusual phenomenon may result from the double-ring envelope, in which at least the new one is in the form of expanding ring. Our results indicate that although both infrared excess and  $H\alpha$  emission line arise from the envelope, their maximum values are likely to reach at the different evolution stage of the envelope.

*Acknowledgements.* We are grateful to Drs D.-M. Wei and H.-C. Wang of Purple Mountain Observatory for their valuable discussion and to Dr J.-Y. Wei and Mr H.-B. Li of Beijing Astronomy Observatory for their assistance in observations. Some data are reduced by Ms J.-P. Xia and Mr Z.-X. Zhu. We also wish to thank an anonymous referee for his/her useful comments and suggestions. QZL acknowledges the financial support from KC Wong fellowship of Chinese Academy of Sciences. This work is partially supported by the Netherlands Organization for Scientific Research (NWO) through Spinoza Grant 08-0 to E.P.J. van den Heuvel and by the National Project for Fundamental Research by the Ministry of Science and Technology of China (973 project).

## References

- Ashok, N.M., Bhatt, H.C., Kulkarni, P.V. et al., 1984, MNRAS, 211, 471
- Braes, L.L.E. & Miley, G.K., 1972, Nature, 235, 273
- Chokshi, A. & Cohen M., 1988, AJ, 94, 123
- Corbet, R.H.D., Thomas, B., 1991, IAUC, 5372
- Dachs, J., Wamsteker, W., 1982, A&A, 107, 579
- Fabregat, J., Reglero, V., Coe, M.J. et al. 1992, A&A, 259, 522
- Hang H.-R., Xia, J.-P., 1995, Acta Astronomia Sinica, 36, 438
- Hanuschik, R.W., Dachs, J., Baudzus, M. et al, 1993, A&A, 274, 356
- Huang, S.-S. , 1972, ApJ, 171, 549
- Huchings, J.B., 1977, MNRAS, 93, 486
- Kastner, J.H. & Mazzali, P.A., 1989, A&A, 210,295
- van Kerkwijk, M.H., Waters, L.B.F.M., & Marlborough, J.M., 1995, A&A, 300, 259
- Kunjaya, C., Hirata, R., 1995, PASJ, 47, 589
- Liu Q.-Z., Hang H.-R., 1997, Acta Astronomia Sinica, 38, 434
- Lyubimkov, L.S., Rostopchin, S.I., Roche, P., Tarasov, A.E., 1997, MNRAS, 286, 549
- Marlborough, J.M., Zijlstra, J.W., & Waters, L.B.F.M., & 1997, A&A, 321, 867
- Mook, D.E., Boley, F.I., Foltz, C.B. et al., 1974, PASP, 86, 894
- Neto, A.D. & Pacheco, J.A. de Freitas, 1982, MNRAS, 198,659
- Norton, A.J., Coe, M.J., Estela, A. et al., 1991, MNRAS, 253, 579
- Osterbrock, D.E, 1989, Astrophysics of Gaseous Nebulae and Active Galactic Nuclei, University Science Books, Mill Valley
- Penrod, G.D. & Vogt, S.S., 1985, ApJ, 299, 653
- Persi, P., Viotti, R., Ferrari-Toniolo, M., 1977, MNRAS, 181, 685
- Reynolds, A.P., Hilditch, R.W., Bell, S.A. et al, 1992, MNRAS, 258, 439
- Roche, P., Coe, M.J., Fabregat, J. et al. 1993, A&A, 270, 122
- Roche, P., Larionov, V., Tarasov, A.E. et al. 1997, A&A, 322, 139
- Tarasov, A.E. & Roche, P., 1995, MNRAS, 276, L19
- Telting, J.H., Waters, L.B.F.M., Roche, P. et al, 1998, MNRAS, 296, 785
- Tucker, W.H., 1975, Radiation processes in astrophysics, MIT Press.
- Waters, L.B.F.M., 1986, A&A, 162, 121
- Waters, L.B.F.M., Taylor, A.R., van den Heuvel, E.P.J. et al., 1988, A&A, 198, 200
- Zamanov, R.K. & Zamanova, V.I., 1995, IBVS, No. 4189